

Asymmetric Diffusion of Chiral Skyrmions

X. Zhang,^{1,*} C. Reichhardt,² C. J. O. Reichhardt,² Y. Zhou,³ Y. Xu,⁴ and M. Mochizuki^{1,†}

¹*Department of Applied Physics, Waseda University, Okubo, Shinjuku-ku, Tokyo 169-8555, Japan*

²*Theoretical Division and Center for Nonlinear Studies, Los Alamos National Laboratory, Los Alamos, New Mexico 87545, USA*

³*School of Science and Engineering, The Chinese University of Hong Kong, Shenzhen, Guangdong 518172, China*

⁴*National Key Laboratory of Spintronics, Nanjing University, Suzhou 215163, China*

(Dated: June 17, 2025)

Brownian dynamics of chiral matter in chiral environment may give rise to emergent phenomena that could not be observed in achiral environment. Here, we report the asymmetric diffusion of chiral skyrmions in two chambers separated by a chiral gate. The topology-determined Brownian gyromotion of skyrmions could lead to effective interactions between skyrmions and chamber walls with a sense of clockwise or counter-clockwise rotation. By fabricating a chiral gate separating two chambers, skyrmions could demonstrate asymmetric diffusion through the gate to approach a nonequilibrium state before reaching the thermal equilibrium. We focus on the asymmetric diffusion of skyrmions that depends on the gate chirality and opening width. Although the simulated diffusion of skyrmions is affected by the skyrmion density, which varies with time due to the diffusion and annihilation, the simulated outcomes are generally in line with simple theories assuming time-independent diffusion rates. Our results uncover asymmetric diffusive behaviors of chiral skyrmions interacting with chiral nanostructures, which will appeal to the wide audience interested in hard condensed matter systems, magnetism, active matter, and statistical physics.

Diffusion is one of the most important phenomena in nature that can be observed at a wide range of length and timescales [1, 2]. It plays a critical role in many key problems in different fields, including physics [3–7], biology [8, 9], and economics [10, 11]. For example, the diffusive transport of particles and particle-like objects is a basic topic in both fundamental research and applied engineering, which covers the flowing phenomena of different phases including gas, liquid, solid, and their mixed phases [12, 13]. In particular, the asymmetric diffusion in artificial nanostructures is essential for functional applications [14–17].

Magnetic skyrmions are a type of topologically non-trivial spin textures that can be treated as particle-like objects with chiral dynamic nature [18–27]. They can be created in chiral magnets, magnetic thin films, and multilayers with antisymmetric exchange interactions [18–27], such magnets with bulk or interfacial Dzyaloshinskii–Moriya (DM) interactions [28–33]. Particularly, skyrmions stabilized by DM interactions have fixed chirality and helicity, which could give rise to unique dynamics induced by external driving forces, such as spin currents [31–37].

Hence, chiral skyrmions could demonstrate various promising transport phenomena due to their unique topology, chirality, and rigidity [18–27]. A famous example is the skyrmion Hall effect, which leads to accumulations of skyrmions at device edges [32, 33, 37]. In addition, skyrmions can demonstrate exotic dynamic behaviors that cannot be reproduced by common particles in gas, liquid, and solid states. For example, many skyrmions may flow in nanochannels and lead to transport phenomena mimicking chiral fluids [37, 38].

Recent reports also suggest that the thermal effects can result in effective diffusion of chiral skyrmions in thin films and layered heterostructures, where skyrmions could show Brownian-type random walk [39–53] and may also demonstrate directional diffusion in the presence of a thermal gra-

dient [54–59]. More interestingly, theoretical and experimental studies have uncovered topology-dependent Brownian gyromotion of skyrmions, which is an emerging effect getting pronounced when diffusive skyrmions are interacting with confinement [60–62]. Such an intriguing topology-determined dynamics may lead to topological sorting phenomena when the confinement environment is also of chiral nature [62]. However, many diffusive features of skyrmions in chiral environment still remain elusive and unexplored, which are essentially important for the functionalization of diffusive skyrmions.

In this *Letter*, we report the asymmetric diffusion of chiral skyrmions at finite temperature but in the absence of thermal gradient. The asymmetry of diffusion is generated by effective but nonsustained interactions between chiral skyrmions and a chiral gate. In Figs. 1(a) and 1(b), we show the system where skyrmions could interact with a chiral gate separating two chambers. The system is a rectangle ferromagnetic monolayer with interface-induced DM interaction and perpendicular magnetic anisotropy (PMA), which has typical magnetic parameters [34, 36, 37, 62]: the saturation magnetization $M_S = 580 \text{ kA m}^{-1}$, exchange constant $A = 15 \text{ pJ m}^{-1}$, PMA constant $K = 0.8 \text{ MJ m}^{-3}$, and DM interaction parameter $D = 3 \text{ mJ m}^{-2}$. The length, width, and thickness of the system are equal to 600 nm, 200 nm, and 1 nm, respectively. By locally enhancing PMA, we could fabricate barrier walls on the ferromagnetic layer [62–65], which form a confined geometry where two chambers with default PMA are separated by a wall with enhanced PMA of $10K$ [Figs. 1(a) and 1(b)]. The barrier wall width (in the x dimension) is fixed at 28 nm. Skyrmions cannot penetrate the barrier wall, however, a gate on the barrier wall with the opening width of W may allow skyrmions to pass through. The gate placed near the upper border forms a chiral gate [Figs. 1(a) and 1(b)], while the gate placed at the center forms an achiral gate [Figs. 1(c) and 1(d)].

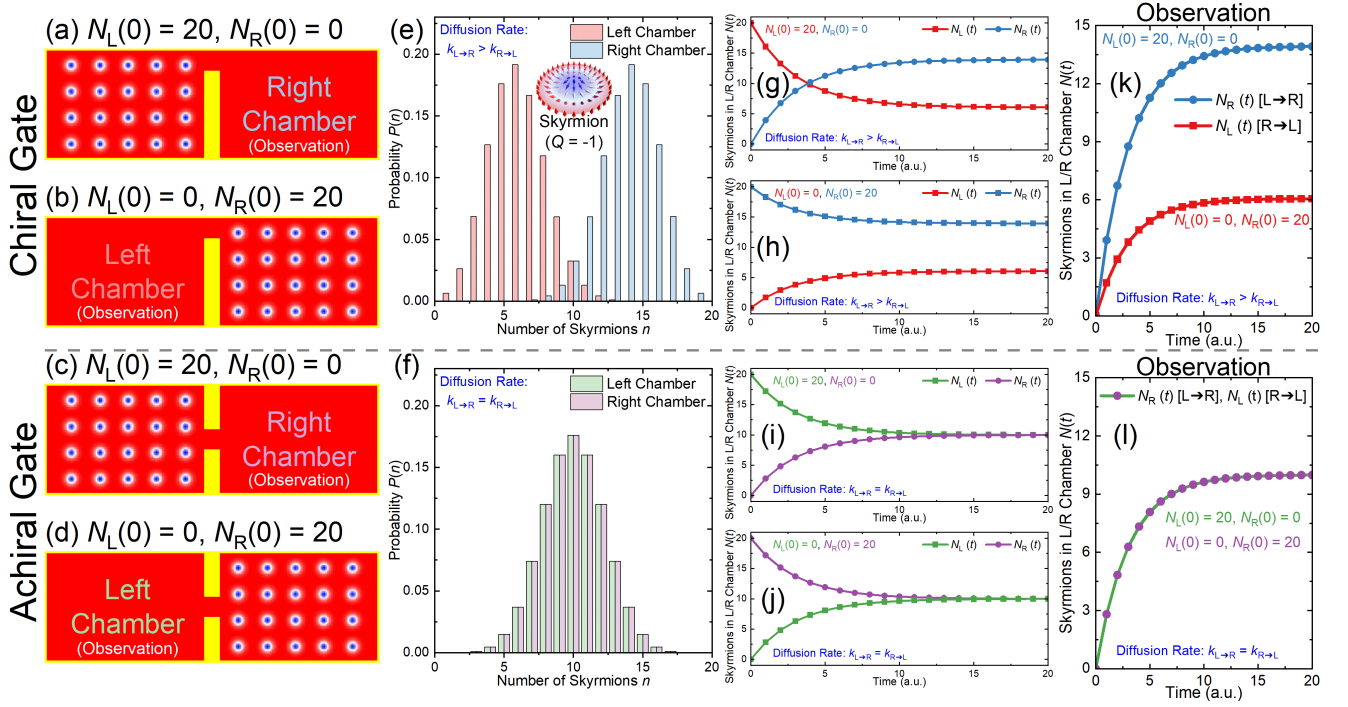


FIG. 1. Theoretical analysis of the probability distribution and diffusion dynamics. (a) Top view of the system with a chiral gate at $t = 0$ ns. The out-of-plane spin component is color coded: blue is into the plane, red is out of the plane, white is in-plane. Initially, 20 chiral skyrmions with $Q = -1$ are placed and relaxed in the left chamber [$N_L(0) = 20$] and no skyrmions are placed in the right chamber [$N_R(0) = 0$]. The chamber walls are indicated by yellow areas. (b) The system with a chiral gate at $t = 0$ ns with $N_L(0) = 0$ and $N_R(0) = 20$. (c) The system with an achiral gate at $t = 0$ ns with $N_L(0) = 20$ and $N_R(0) = 0$. (d) The system with an achiral gate at $t = 0$ ns with $N_L(0) = 0$ and $N_R(0) = 20$. (e) Probability distribution of the system with a chiral gate, assuming that the diffusion rate $k_{L \rightarrow R} = 0.23$ and $k_{R \rightarrow L} = 0.1$ as skyrmions with $Q = -1$ showing clockwise gyromotion is easier to pass through the given chiral gate from the left, i.e., $k_{L \rightarrow R} > k_{R \rightarrow L}$. Inset shows a schematic illustration of the skyrmion with $Q = -1$. (f) Probability distribution of the system with an achiral gate, assuming the diffusion rate $k_{L \rightarrow R} = k_{R \rightarrow L} = 0.165$. (g) Time-dependent numbers of skyrmions in the left [$N_L(t)$] and right [$N_R(t)$] chambers separated by a chiral gate. Here, $N_L(0) = 20$ and $N_R(0) = 0$. (h) $N_L(t)$ and $N_R(t)$ of the system with a chiral gate, where $N_L(0) = 0$ and $N_R(0) = 20$. (i) $N_L(t)$ and $N_R(t)$ of the system with an achiral gate, where $N_L(0) = 20$ and $N_R(0) = 0$. (j) $N_L(t)$ and $N_R(t)$ of the system with an achiral gate, where $N_L(0) = 0$ and $N_R(0) = 20$. (k) Time-dependent $N_R(L \rightarrow R)$ and $N_L(R \rightarrow L)$ of the system with a chiral gate. (l) Time-dependent $N_R(L \rightarrow R)$ and $N_L(R \rightarrow L)$ of the system with an achiral gate.

In this work, we focus on the diffusive behaviors of skyrmions carrying the topological charge of $Q = \frac{1}{4\pi} \int \mathbf{m} \cdot (\frac{\partial \mathbf{m}}{\partial x} \times \frac{\partial \mathbf{m}}{\partial y}) dx dy = -1$. The Brownian dynamics of a skyrmion is associated with its Q [60], especially when the skyrmion is thermally interacting with confining potentials in the absence of thermal gradients [62]. For example, a skyrmion with $Q = -1$ stabilized by interface-induced DM interaction has a clockwise sense of rotation during its Brownian gyromotion [60, 62]. Therefore, the skyrmion with $Q = -1$ is in principle easier to pass through the given chiral gate [Fig. 1(a)] from the left chamber provided that the opening width W is appropriate. It is also expected that the possibility to pass through an achiral gate [Fig. 1(c)] should be identical for the left-to-right ($L \rightarrow R$) and right-to-left ($R \rightarrow L$) cases.

We first analyze possible diffusive behaviors in the chiral and achiral systems from the viewpoint of thermodynamics [66]. We consider 20 skyrmions in the left or right chamber as the initial condition, and assume a simplified system with a fixed temperature and no thermal annihilation of skyrmions.

We also assume that the interactions between skyrmions and the gate are always effective and do not depend on other factors, such as the skyrmion density. Thus, the diffusion rate of skyrmions is treated as a time-independent parameter. As skyrmions with $Q = -1$ are easier to pass through the chiral gate from the left chamber, the diffusion rate $k_{L \rightarrow R}$ should be larger than $k_{R \rightarrow L}$, where “ $L \rightarrow R$ ” denotes that skyrmions diffuse from the left to the right chamber, and “ $R \rightarrow L$ ” denotes that skyrmions diffuse from the right to the left chamber. Here, we assume $k_{L \rightarrow R} = 0.23$ and $k_{R \rightarrow L} = 0.1$.

Therefore, the equilibrium probability distribution of skyrmions in the left chamber equals $P(n) = \Omega(n) p_L^n (p_R)^{N-n}$, where $p_L = k_{R \rightarrow L} / (k_{L \rightarrow R} + k_{R \rightarrow L})$ and $p_R = k_{L \rightarrow R} / (k_{L \rightarrow R} + k_{R \rightarrow L}) = 1 - p_L$ are the probabilities of a skyrmion being in the left and right chamber, respectively. $\Omega(n) = N! / [n!(N-n)!]$ represents the number of microstates when the number of skyrmions in the left chamber $N_L = n$. $N = N_T = 20$ is the total number of skyrmions in the system. In Fig. 1(e), it shows that the asymmetric

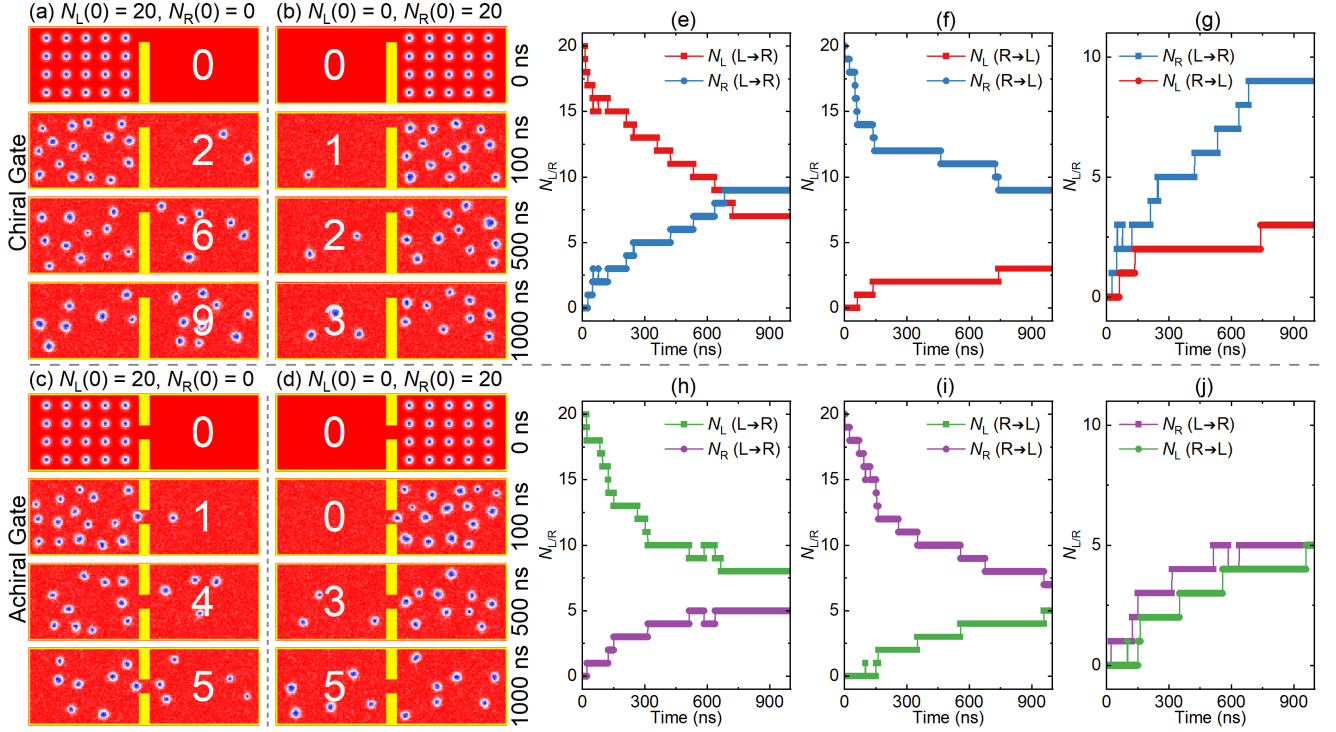


FIG. 2. Simulated diffusion of chiral skyrmions interacting with a chiral or achiral gate. (a) Selected top-view snapshots of the system with a chiral gate, where $N_L(0) = 20$ and $N_R(0) = 0$. (b) Selected top-view snapshots of the system with a chiral gate, where $N_L(0) = 0$ and $N_R(0) = 20$. (c) Selected top-view snapshots of the system with an achiral gate, where $N_L(0) = 20$ and $N_R(0) = 0$. (d) Selected top-view snapshots of the system with an achiral gate, where $N_L(0) = 0$ and $N_R(0) = 20$. (e) Time-dependent $N_L(L \rightarrow R)$ and $N_R(L \rightarrow R)$ and (f) time-dependent $N_L(R \rightarrow L)$ and $N_R(R \rightarrow L)$ of the simulated system with a chiral gate. Time-dependent $N_R(L \rightarrow R)$ and $N_L(R \rightarrow L)$ of the observation chamber are given in (g). (h) Time-dependent $N_L(L \rightarrow R)$ and $N_R(L \rightarrow R)$ and (i) time-dependent $N_L(R \rightarrow L)$ and $N_R(R \rightarrow L)$ of the simulated system with an achiral gate. Time-dependent $N_R(L \rightarrow R)$ and $N_L(R \rightarrow L)$ of the observation chamber are given in (j). All simulations are performed with parameters: $W = 36$ nm, $T = 150$ K, and $S = 304$.

diffusion $k_{L \rightarrow R} > k_{R \rightarrow L}$ leads to different equilibrium distributions of skyrmions, where more skyrmions can be found in the right chamber at equilibrium. However, for symmetric diffusion $k_{L \rightarrow R} = k_{R \rightarrow L} = 0.165$, for example, the equilibrium distributions of skyrmions are identical in the left and right chambers [Fig. 1(f)].

In Fig. 1(g), we show the theoretical diffusion if a total number of $N_L(0) = N_T = 20$ skyrmions are placed in the left chamber initially (i.e., no skyrmions in the right chamber). The diffusion equations for the number of skyrmions in the left and right chambers read $N_L(t) = p_L N_T + (N_T - p_L N_T) e^{-(k_{L \rightarrow R} + k_{R \rightarrow L})t}$ and $N_R(t) = N_T - N_L(t)$, respectively. The case with $N_L(0) = 0$ and $N_R(0) = N_T = 20$ is given in Fig. 1(h). On the other hand, the diffusion behaviors for skyrmions interacting with an achiral gate ($k_{L \rightarrow R} = k_{R \rightarrow L}$) are given in Figs. 1(i) and 1(j).

If we focus on the initially empty chamber and observe the skyrmions diffused to it within a fixed period of time, we could find asymmetric diffusion for skyrmions interacting with a chiral gate ($k_{L \rightarrow R} > k_{R \rightarrow L}$), where more skyrmions can escape from the left chamber [Fig. 1(k)] within the same time. However, for skyrmions interacting with an achiral gate ($k_{L \rightarrow R} = k_{R \rightarrow L}$), the diffusion is symmetric and one can find

the same amount of escaped skyrmions within the same time [Fig. 1(l)].

To examine the theoretical predictions, we carried out computational experiments by simulating the spin dynamics of the entire system using the MuMax³ simulator [67]. We consider spin dynamics at finite temperature governed by the stochastic Landau-Lifshitz-Gilbert equation, and we include the ferromagnetic exchange, interface-induced DM interaction, PMA, and demagnetization energy terms in all simulations (see [Supplementary Note 1](#)) [68].

In Figs. 2(a) and 2(b), we show simulated diffusion of skyrmions with $Q = -1$ interacting with a chiral gate (see [Supplementary Videos 1 and 2](#)) [68]. We assume $W = 36$ nm and $T = 150$ K with a thermal random seed of $S = 304$. At $t = 0$ ns, 20 skyrmions with $Q = -1$ are placed and relaxed in either the left or right chamber. For the case with $N_L(0) = 20$ and $N_R(0) = 0$, we find $N_R = 9$ at $t = 1000$ ns, and we find $N_L = 3$ at $t = 1000$ ns for the case with $N_L(0) = 0$ and $N_R(0) = 20$. These observation results indicate the diffusion of skyrmions interacting with a chiral gate is asymmetric. In contrast, the observation of the system with an achiral gate indicates a nearly symmetric diffusion (see [Supplementary Videos 3 and 4](#)) [68], as we find that 5

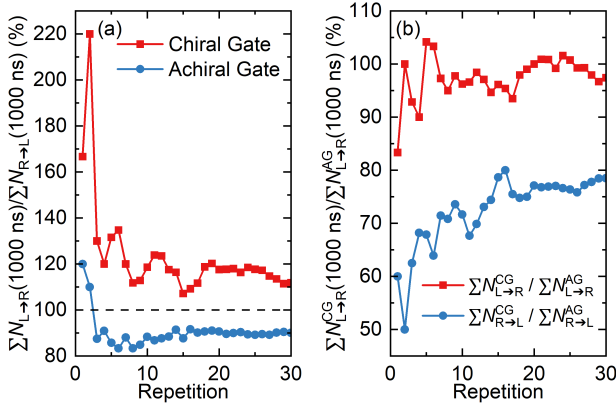


FIG. 3. Repetition dependence of the simulated outcomes. (a) Summation of the number of skyrmions in the right observation chamber ($\sum_S N_{L \rightarrow R}$) over that in the left observation chamber ($\sum_S N_{R \rightarrow L}$) obtained at $t = 1000$ ns for 30 repetitions of the same simulation with different seeds S . (b) $\sum_S N_{L \rightarrow R}^{\text{CG}}$ (or $\sum_S N_{R \rightarrow L}^{\text{CG}}$) of the system with a chiral gate over $\sum_S N_{L \rightarrow R}^{\text{AG}}$ (or $\sum_S N_{R \rightarrow L}^{\text{AG}}$) of the system with an achiral gate, obtained at $t = 1000$ ns for 30 repetitions of the same simulation with different seeds S . Other parameters are fixed: $W = 36$ nm and $T = 150$ K.

skyrmions could diffuse within 1000 ns to the initially empty chamber from the left or right chamber initially filled with 20 skyrmions [Figs. 2(c) and 2(d)].

In Figs. 2(e) and 2(f), we show $N_L(t)$ and $N_R(t)$ corresponding to the systems given in Figs. 2(a) and 2(b) for 1000-ns-long simulations with the same parameters, respectively. $N_L(L \rightarrow R)$ and $N_R(L \rightarrow R)$ represent the number of skyrmions in the left and right chambers, respectively, during the left-to-right ($L \rightarrow R$) diffusion process, where skyrmions initially placed in the left chamber diffuse into the right chamber [Figs. 2(a) and 2(c)]. Conversely, $N_L(R \rightarrow L)$ and $N_R(R \rightarrow L)$ indicate the number of skyrmions in each chamber during the right-to-left ($R \rightarrow L$) diffusion process [Figs. 2(b) and 2(d)]. By comparing $N_R(L \rightarrow R)$ and $N_L(R \rightarrow L)$, the asymmetric diffusion of skyrmions in the chiral system is confirmed [Fig. 2(g)], which is in line with the theoretical trend [Fig. 1(k)]. For the achiral system, $N_R(L \rightarrow R)$ is very close to $N_L(R \rightarrow L)$ [Fig. 2(j)], which agrees with the theoretical trend [Fig. 1(l)].

It should be noted that the total number of skyrmions in simulations is decreasing with time due to thermal annihilation (see Supplementary Fig. 1) [68], which could reduce the skyrmion density and affect the observation results. The diffusion rate depends on the skyrmion density that affects the effectiveness of skyrmion-gate and skyrmion-skyrmion interactions, therefore, it is expected that the diffusion rates $k_{L \rightarrow R}$ and $k_{R \rightarrow L}$ in simulations are time-dependent and may approach the same value even if they start from $k_{L \rightarrow R} > k_{R \rightarrow L}$ at $t = 0$ ns. Furthermore, since skyrmions have a finite size and interact through short-range repulsive forces, an excessively high skyrmion density in the chamber at $t = 0$ ns could lead to strong skyrmion-skyrmion repulsion. This repulsion

may cause skyrmions to be expelled from the chamber during the early stages of diffusion, without showing an effective interaction with the gate. In our model, the initial state of 20 skyrmions in either the left or right chamber results in a moderate initial density that ensures $k_{L \rightarrow R} > k_{R \rightarrow L}$ from $t = 0$ ns. In Supplementary Fig. 2 [68], we show the opening width W of the chiral gate will also affect the observed outcome as the skyrmion-gate interaction delicately depends on the ratio between the skyrmion size and W .

We also performed 30 repetitions of the simulations demonstrated in Fig. 2 with the same parameters but different thermal random seeds S . In Fig. 3(a), we show the summation of the number of skyrmions observed at $t = 1000$ ns in the initially empty right chamber $\sum_S N_R(L \rightarrow R)$ over that in the initially empty left chamber $\sum_S N_L(R \rightarrow L)$. For the system with a chiral gate, we find $\sum_S N_R(L \rightarrow R) / \sum_S N_L(R \rightarrow L) > 1$ for 30 repetitions, justifying the asymmetric diffusion (see also Supplementary Fig. 3) [68]. However, for the achiral system, we find $\sum_S N_R(L \rightarrow R) / \sum_S N_L(R \rightarrow L)$ decreases from ~ 1.2 to ~ 0.8 and then approaches ~ 0.9 , suggesting that the skyrmions interacting with the achiral gate show a slightly asymmetric diffusion (i.e., unbalanced outcomes) for 30 repetitions of the simulation, which we believe may be caused by short-term randomness. In principle, one should find $\sum_S N_R(L \rightarrow R) / \sum_S N_L(R \rightarrow L) \sim 1$ for the achiral system if a sufficiently large number of repetitions are done.

We also compare $\sum_S N_R^{\text{CG}}(L \rightarrow R)$ of the system with a chiral gate with $\sum_S N_R^{\text{AG}}(L \rightarrow R)$ of the system with an achiral gate [Fig. 3(b)]. $\sum_S N_R^{\text{CG}}(L \rightarrow R) / \sum_S N_R^{\text{AG}}(L \rightarrow R)$ is generally smaller than 1, which means the skyrmions are easier to pass through the achiral gate compared to the chiral gate system. This reason is that the achiral gate is positioned at the system center, whereas the chiral gate is located near the upper border. Consequently, skyrmions are more likely to interact with the achiral gate than with the chiral gate. Such a trend is pronounced when more repetitions are performed (see Supplementary Fig. 3) [68]. On the other hand, the value of $\sum_S N_R^{\text{CG}}(L \rightarrow R) / \sum_S N_R^{\text{AG}}(L \rightarrow R)$ is obviously larger than that of $\sum_S N_L^{\text{CG}}(R \rightarrow L) / \sum_S N_L^{\text{AG}}(R \rightarrow L)$, which justifies again that the skyrmions with $Q = -1$ are easier to diffuse from the left chamber to the right chamber through the chiral gate.

In conclusion, we have evidenced the asymmetric diffusion of chiral skyrmions interacting with a chiral gate. Such a highly nontrivial dynamic phenomenon is a result of the Brownian gyromotion reflecting the topological nature of skyrmions, as well as the effective interactions between chiral skyrmions and chiral structures. The skyrmion-gate interaction and the consequence diffusion asymmetry depend on many factors, such as the gate chirality, gate opening width, and skyrmion density. The gate cannot be modified once fabricated but skyrmion density and size are subject to thermal effects, for example. Because the diffusion rate in real system is varying and dependent of the skyrmion density, the simulated system may not reach a sustained nonequilibrium steady state but could create time-dependent nonequilibrium phenomena

before it reaches thermal equilibrium driven by the increasing entropy of the entire system. This work paves the way for the study of complex diffusion behaviors of chiral magnetic matter, which may be useful for building nonconventional computing devices based on diffusion asymmetry. We also note that our results should be relevant to other systems where chiral diffusion can occur [69–72], such as various types of chiral active matter systems, systems with chiral nonreciprocal interactions, systems with odd viscosity, and certain charged systems in magnetic fields.

X.Z. and M.M. acknowledge support by the CREST, the Japan Science and Technology Agency (Grant No. JP-MJCR20T1). X.Z. also acknowledges support by the Grants-in-Aid for Scientific Research from JSPS KAKENHI (Grant No. JP25K17939 and No. JP20F20363). M.M. also acknowledges support by the Grants-in-Aid for Scientific Research from JSPS KAKENHI (Grants No. JP25H00611, No. JP24H02231, No. JP23H04522, and No. JP20H00337) and the Waseda University Grant for Special Research Projects (Grant No. 2025C-133). C.R. and C.J.O.R. acknowledge the support by the U.S. Department of Energy through the Los Alamos National Laboratory. Los Alamos National Laboratory is operated by Triad National Security, LLC, for the National Nuclear Security Administration of the U.S. Department of Energy (Contract No. 892333218NCA000001). Y.Z. acknowledges support by the Shenzhen Fundamental Research Fund (Grant No. JCYJ20210324120213037), the Guangdong Basic and Applied Basic Research Foundation (Grant No. 2021B1515120047), the Shenzhen Peacock Group Plan (Grant No. KQTD20180413181702403), the National Natural Science Foundation of China (Grant No. 12374123), and the 2023 SZSTI Stable Support Scheme.

* Email: xichaozhang@aoni.waseda.jp

† Email: masa_mochizuki@waseda.jp

- [1] J. Philibert, *Diffus. Fundam.* **4**(6), 1 (2006).
- [2] H. Mehrer and N. A. Stolwijk, *Diffus. Fundam.* **11**(1), 1 (2009).
- [3] P. M. Fahey, P. B. Griffin, and J. D. Plummer, *Rev. Mod. Phys.* **61**, 289 (1989).
- [4] O. Firtenberg, M. Shuker, A. Ron, and N. Davidson, *Rev. Mod. Phys.* **85**, 941 (2013).
- [5] P. Huber, *J. Phys.: Condens. Matter* **27**, 103102 (2015).
- [6] N. Masuda, M. A. Porter, and R. Lambiotte, *Phys. Rep.* **716–717**, 1 (2017).
- [7] F. Yang, Z. Zhang, L. Xu, Z. Liu, P. Jin, P. Zhuang, M. Lei, J. Liu, J.-H. Jiang, X. Ouyang, F. Marchesoni, and J. Huang, *Rev. Mod. Phys.* **96**, 015002 (2024).
- [8] T. Chou, K. Mallick, and R. K. P. Zia, *Rep. Prog. Phys.* **74**, 116601 (2011).
- [9] L. M. Ricciardi, *Diffusion processes and related topics in biology*, Vol. 14. (Springer Science and Business Media, 2013).
- [10] B. H. Hall, National Bureau of Economic Research Working Paper Series, No. 10212 (2004).
- [11] B. Kogut and J. M. Macpherson, *Res. Policy* **40**, 1307 (2011).
- [12] S. Park, J.-W. Lee, and B. N. Popov, *Int. J. Hydrog. Energy* **37**, 5850 (2012).
- [13] R. J. Borg and G. J. Dienes, *An introduction to solid state diffusion* (Elsevier, 2012).
- [14] N. Packard and R. Shaw, *arXiv:cond-mat/0412626* (2005).
- [15] Z. Siwy, I. D. Kosinska, A. Fulinski, and C. R. Martin, *Phys. Rev. Lett.* **94**, 048102 (2005).
- [16] R.S. Shaw, N. Packard, M. Schroter, and H. L. Swinney, *Proc. Natl. Acad. Sci. U.S.A.* **104**, 9580 (2007).
- [17] Z. Xu, D. Zheng, B. Ai, and W. Zhong, *Sci. Rep.* **6**, 23414 (2016).
- [18] M. Mochizuki and S. Seki, *J. Phys.: Condens. Matter* **27**, 503001 (2015).
- [19] G. Finocchio, F. Büttner, R. Tomasello, M. Carpentieri, and M. Kläui, *J. Phys. D: Appl. Phys.* **49**, 423001 (2016).
- [20] R. Wiesendanger, *Nat. Rev. Mat.* **1**, 16044 (2016).
- [21] A. Fert, N. Reyren, and V. Cros, *Nat. Rev. Mater.* **2**, 17031 (2017).
- [22] W. Jiang, G. Chen, K. Liu, J. Zang, S. G. Velthuis, and A. Hoffmann, *Phys. Rep.* **704**, 1 (2017).
- [23] X. Zhang, Y. Zhou, K. M. Song, T.-E. Park, J. Xia, M. Ezawa, X. Liu, W. Zhao, G. Zhao, and S. Woo, *J. Phys. Condens. Matter* **32**, 143001 (2020).
- [24] B. Göbel, I. Mertig, and O. A. Tretiakov, *Phys. Rep.* **895**, 1 (2021).
- [25] N. Del-Valle, J. Castell-Queralt, L. González-Gómez, and C. Navau, *APL Mater.* **10**, 010702 (2022).
- [26] C. Reichhardt, C. J. O. Reichhardt, and M. V. Milosevic, *Rev. Mod. Phys.* **94**, 035005 (2022).
- [27] Y. Ohki and M. Mochizuki, *J. Phys.: Condens. Matter* **37**, 023003 (2024).
- [28] U. K. Röbler, A. N. Bogdanov, and C. Pfleiderer, *Nature* **442**, 797 (2006).
- [29] S. Mühlbauer, B. Binz, F. Jonietz, C. Pfleiderer, A. Rosch, A. Neubauer, R. Georgii, and P. Böni, *Science* **323**, 915 (2009).
- [30] X. Z. Yu, Y. Onose, N. Kanazawa, J. H. Park, J. H. Han, Y. Matsui, N. Nagaosa, and Y. Tokura, *Nature* **465**, 901 (2010).
- [31] W. Jiang, P. Upadhyaya, W. Zhang, G. Yu, M. B. Jungfleisch, F. Y. Fradin, J. E. Pearson, Y. Tserkovnyak, K. L. Wang, O. Heinonen, S. G. E. te Velthuis, and A. Hoffmann, *Science* **349**, 283 (2015).
- [32] W. Jiang, X. Zhang, G. Yu, W. Zhang, X. Wang, M. Benjamin Jungfleisch, J. E. Pearson, X. Cheng, O. Heinonen, K. L. Wang, Y. Zhou, A. Hoffmann, and S. G. E. Velthuis, *Nat. Phys.* **13**, 162 (2017).
- [33] K. Litzius, I. Lemesh, B. Kruger, P. Bassirian, L. Caretta, K. Richter, F. Büttner, K. Sato, O. A. Tretiakov, J. Forster, R. M. Reeve, M. Weigand, I. Bykova, H. Stoll, G. Schutz, G. S. D. Beach, and M. Kläui, *Nat. Phys.* **13**, 170 (2017).
- [34] R. Tomasello, E. Martinez, R. Zivieri, L. Torres, M. Carpentieri, and G. Finocchio, *Sci. Rep.* **4**, 6784 (2014).
- [35] C. Reichhardt and C. J. O. Reichhardt, *Nat. Commun.* **11**, 738 (2020).
- [36] X. Zhang, J. Xia, and X. Liu, *Phys. Rev. B* **106**, 094418 (2022).
- [37] X. Zhang, J. Xia, O. A. Tretiakov, M. Ezawa, G. Zhao, Y. Zhou, X. Liu, and M. Mochizuki, *Phys. Rev. B* **108**, 144428 (2023).
- [38] K. Raab, M. Schmitt, M. A. Brems, J. Rothorl, F. Kammerbauer, S. Krishna, M. Kläui, and P. Virnau, *Phys. Rev. E* **110**, L042601 (2024).
- [39] R. E. Troncoso and A. S. Núñez, *Ann. Phys.* **351**, 850 (2014).
- [40] C. Schütte, J. Iwasaki, A. Rosch, and N. Nagaosa, *Phys. Rev. B* **90**, 174434 (2014).
- [41] J. Barker and O. A. Tretiakov, *Phys. Rev. Lett.* **116**, 147203 (2016).
- [42] J. Miltat, S. Rohart, and A. Thiaville, *Phys. Rev. B* **97**, 214426 (2018).

- [43] T. Nozaki, Y. Jibiki, M. Goto, E. Tamura, T. Nozaki, H. Kubota, A. Fukushima, S. Yuasa, and Y. Suzuki, *Appl. Phys. Lett.* **114**, 012402 (2019).
- [44] M. Weißenhofer and U. Nowak, *New J. Phys.* **22**, 103059 (2020).
- [45] K. Y. Jing, C. Wang, and X. R. Wang, *Phys. Rev. B* **103**, 174430 (2021).
- [46] Y. Zhou, R. Mansell, T. Ala-Nissila, and S. van Dijken, *Phys. Rev. B* **104**, 144417 (2021).
- [47] Y. Suzuki, S. Miki, Y. Imai, and E. Tamura, *Phys. Lett. A* **413**, 127603 (2021).
- [48] R. Ishikawa, M. Goto, H. Nomura, and Y. Suzuki, *Appl. Phys. Lett.* **119**, 072402 (2021).
- [49] M. Weißenhofer, L. Rózsa, and U. Nowak, *Phys. Rev. Lett.* **127**, 047203 (2021).
- [50] N. Kerber, M. Weißenhofer, K. Raab, K. Litzius, J. Zázvorka, U. Nowak, and M. Kläui, *Phys. Rev. Applied* **15**, 044029 (2021).
- [51] M. Weißenhofer and U. Nowak, *Phys. Rev. B* **107**, 064423 (2023).
- [52] R. Gruber, M. A. Brems, J. Rothörl, T. Sparmann, M. Schmitt, I. Kononenko, F. Kammerbauer, M.-A. Syskaki, O. Farago, P. Virnau, and M. Kläui, *Adv. Mater.* **35**, 2208922 (2023).
- [53] T. Dohi, M. Weißenhofer, N. Kerber, F. Kammerbauer, Y. Ge, K. Raab, J. Zázvorka, M.-A. Syskaki, A. Shahee, M. Ruhwedel, T. Böttcher, P. Pirro, G. Jakob, U. Nowak, and M. Kläui, *Nat. Commun.* **14**, 5424 (2023).
- [54] L. Kong and J. Zang, *Phys. Rev. Lett.* **111**, 067203 (2013).
- [55] S. Z. Lin, C. D. Batista, C. Reichhardt, and A. Saxena, *Phys. Rev. Lett.* **112**, 187203 (2014).
- [56] C. Reichhardt and C. J. O. Reichhardt, *New J. Phys.* **18**, 095005 (2016).
- [57] C. Reichhardt and C. J. O. Reichhardt, *J. Phys.: Condens. Matter* **31**, 07LT01 (2019).
- [58] Z. Wang, M. Guo, H. A. Zhou, L. Zhao, T. Xu, R. Tomasello, H. Bai, Y. Dong, S. G. Je, W. Chao, H. S. Han, S. Lee, K. S. Lee, Y. Yao, W. Han, C. Song, H. Wu, M. Carpentieri, G. Finocchio, M. Y. Im, S. Z. Lin, and W. Jiang, *Nat. Electron.* **3**, 672 (2020).
- [59] L. Kong, X. Chen, W. Wang, D. Song, and H. Du, *Phys. Rev. B* **104**, 214407 (2021).
- [60] L. Zhao, Z. Wang, X. Zhang, X. Liang, J. Xia, K. Wu, H. A. Zhou, Y. Dong, G. Yu, K. L. Wang, X. Liu, Y. Zhou, and W. Jiang, *Phys. Rev. Lett.* **125**, 027206 (2020).
- [61] S. Miki, Y. Jibiki, E. Tamura, M. Goto, M. Oogane, J. Cho, R. Ishikawa, H. Nomura, and Y. Suzuki, *J. Phys. Soc. Jpn.* **90**, 083601 (2021).
- [62] X. Zhang, J. Xia, O. A. Tretiakov, M. Ezawa, G. Zhao, Y. Zhou, X. Liu, and M. Mochizuki, *Nano Lett.* **23**, 11793 (2023).
- [63] R. Juge, K. Bairagi, K. G. Rana, J. Vogel, M. Sall, D. Mailly, V. T. Pham, Q. Zhang, N. Sisodia, M. Foerster, L. Aballe, M. Belmeguenai, Y. Roussigné, S. Auffret, L. D. Buda-Prejbeanu, G. Gaudin, D. Ravelosona, and O. Boulle, *Nano Lett.* **21**, 2989 (2021).
- [64] K. Ohara, X. Zhang, Y. Chen, Z. Wei, Y. Ma, J. Xia, Y. Zhou, and X. Liu, *Nano Lett.* **21**, 4320 (2021).
- [65] X. Zhang, J. Xia, K. Shirai, H. Fujiwara, O. A. Tretiakov, M. Ezawa, Y. Zhou, and X. Liu, *Commun. Phys.* **4**, 255 (2021).
- [66] H. Callen, *Thermodynamics and an Introduction to Thermo-statistics* (New York: John Wiley and Sons, 1985).
- [67] A. Vansteenkiste, J. Leliaert, M. Dvornik, M. Helsen, F. Garcia-Sanchez, and B. V. Waeyenberge, *AIP Adv.* **4**, 107133 (2014).
- [68] See Supplemental Material at [\[URL\]](#) for supplementary figures and supplemental videos showing the diffusion of chiral skyrmions interacting with a chiral or achiral gate.
- [69] B. C. van Zuiden, J. Paulose, W. T. M. Irvine, D. Bartolo, and V. Vitelli, *Proc. Natl. Acad. Sci. USA* **113**, 12919 (2016).
- [70] D. Banerjee, A. Souslov, A. G. Abanov, and V. Vitelli, *Nat. Commun.* **8**, 1573 (2017).
- [71] M. Fruchart, R. Hanai, P. B. Littlewood, and V. Vitelli, *Nature* **592**, 363 (2021).
- [72] M. Fruchart, C. Scheibner, and V. Vitelli, *Annu. Rev. Condens. Matter Phys.* **14**, 471 (2023).